

# JAAS

Accepted Manuscript



This is an *Accepted Manuscript*, which has been through the Royal Society of Chemistry peer review process and has been accepted for publication.

*Accepted Manuscripts* are published online shortly after acceptance, before technical editing, formatting and proof reading. Using this free service, authors can make their results available to the community, in citable form, before we publish the edited article. We will replace this *Accepted Manuscript* with the edited and formatted *Advance Article* as soon as it is available.

You can find more information about *Accepted Manuscripts* in the [Information for Authors](#).

Please note that technical editing may introduce minor changes to the text and/or graphics, which may alter content. The journal's standard [Terms & Conditions](#) and the [Ethical guidelines](#) still apply. In no event shall the Royal Society of Chemistry be held responsible for any errors or omissions in this *Accepted Manuscript* or any consequences arising from the use of any information it contains.

**Accumulation and spatial distribution of arsenic and phosphorus in the fern***Pityrogramma calomelanos* evaluated by micro X-Ray fluorescence spectrometry

Naiara Viana Campos<sup>a</sup>, Marcelo Braga Bueno Guerra<sup>b,c\*</sup>, Jaime Wilson V. Mello<sup>c</sup>,  
Carlos Ernesto G. R. Schaefer<sup>c</sup>, Francisco José Krug<sup>b</sup>, Elton E. N. Alves<sup>c</sup>, Aristéa A.  
Azevedo<sup>a</sup>

<sup>a</sup>Department of Plant Biology, Universidade Federal de Viçosa, Av. Peter Henry Rolfs,  
36570-900 Viçosa, MG, Brazil.

<sup>b</sup>Center for Nuclear Energy in Agriculture, Research Support Center “Technology and  
Innovation for a Sustainable Agriculture”, University of São Paulo, Av. Centenário 303,  
13416-000 Piracicaba, SP, Brazil.

<sup>c</sup>Department of Soil Science, Universidade Federal de Viçosa, Av. Peter Henry Rolfs,  
36570-900 Viçosa, MG, Brazil.

\*Corresponding author, e-mail: marcelobbg@gmail.com; Tel.: +55 19 3429-4648

**Abstract**

The accumulation and spatial distribution of arsenic and phosphorus in the As-hyperaccumulator fern *Pityrogramma calomelanos* were investigated with micro-energy dispersive X-ray fluorescence spectrometry ( $\mu$ -EDXRF). Ferns were grown in half-strength Hoagland nutrient solution without and with 1.0, 10 or 30  $\times 10^{-3}$  mol L<sup>-1</sup> As during three weeks. Microchemical As and P maps in different areas of the pinna were obtained by  $\mu$ -EDXRF, and the same elements were also determined in pelletized powdered samples from the pinna, stipe and root. The reference method for the determination of As and P in the fern samples was a validated method based on microwave-assisted acid digestion followed by ICP OES analysis. Correlations between X-ray characteristic emission intensities and the corresponding As and P mass fractions obtained from the analysis of pelletized test samples exhibited linear correlation coefficients higher than 0.98 (n = 42). Better root mean square errors of prediction (RMSEP) were obtained when different calibration models were built with pinna, stipe and root test samples separately. Arsenic was accumulated mainly in the pinna midrib, secondary veins, and apical and marginal regions of the pinnule of *P. calomelanos*, causing alterations in the P distribution. The proposed  $\mu$ -EDXRF method is an appropriate analytical tool for simultaneously mapping As and P in *P. calomelanos*. In addition, useful information for either environmental monitoring or phytoremediation studies regarding As contamination is properly obtained.

**Keywords**

EDXRF, Elemental mapping, As-hyperaccumulator, plant nutrition, phytoremediation.

## Introduction

Arsenic, recognized as a potential contaminant of great concern, is worldwide distributed in nature, mainly as arsenopyrite (FeAsS), the most common arsenic mineral.<sup>1</sup> Parent materials containing arsenopyrite and other As-bearing sulfides are oxidized when exposed to atmospheric oxygen and water, thus releasing this potentially toxic element.<sup>2</sup> This natural phenomenon is called acid mine drainage<sup>3,4</sup> and it is the main cause of high As levels in freshwater reservoirs.<sup>2</sup> Anthropogenic activities, such as the intensive use of arsenical pesticides, mining, fossil-fuel burning and disposal of As-enriched wastes, can also substantially enhance the As contamination.<sup>5</sup> High arsenic levels in soil and groundwater may lead to deleterious effects to the ecosystem, and efforts towards environmental monitoring and remediation programs must be implemented in order to minimize the organisms' exposure to this element.<sup>6-8</sup>

Plants naturally growing in metal(loid)-contaminated soils are adapted to survive in this stressful environment and are classified into three main categories: metal excluders, indicators and accumulators/hyperaccumulators.<sup>9</sup> The majority of plant species are excluders, which contain low levels of potentially toxic elements in their aerial tissues, even when exposed to higher concentrations of contaminants. Indicators present metal(loid)s into their aboveground biomass, thus reflecting the elemental concentration in the soil. Accumulators/hyperaccumulators are able to increase metal(loid) internal sequestration, translocation and accumulation into their fronds to levels that far exceed those usually found in the soil.<sup>9,10</sup>

Arsenic-hyperaccumulator species, *e.g.* *Pteris vittata*<sup>11</sup> and *Pityrogramma calomelanos*<sup>12</sup> differ from As-accumulators by having metalloid mass fractions higher than 1 % m m<sup>-1</sup> dry matter. These hyperaccumulator plants are promising organisms in environmental monitoring and in remediation programs.<sup>13,14</sup> In this sense, arsenic

1  
2  
3 concentration in leaves of hyperaccumulators can be taken into account for evaluating  
4  
5 the input of As in the soil/water system by natural/anthropogenic sources. These plants  
6  
7 can be harvested to reduce potential As contamination, thereby limiting the metalloid  
8  
9 entry into the food chain, a strategy known as phytoremediation.<sup>15</sup>  
10

11  
12 In environmental studies, the quantitative determination of trace elements in plant  
13  
14 materials has been generally accomplished by atomic absorption spectrometry (flame,  
15  
16 graphite furnace, hydride generation), inductively coupled plasma (ICP) optical  
17  
18 emission spectrometry or ICP-mass spectrometry.<sup>16,17</sup> These methods often require an *a*  
19  
20 *priori* chemical treatment for the decomposition of the organic material, usually  
21  
22 involving microwave-assisted digestion with nitric acid and hydrogen peroxide.<sup>18-20</sup>  
23  
24 Micro-energy dispersive X-ray fluorescence spectrometry ( $\mu$ -EDXRF) is a fast and non-  
25  
26 destructive method that has been successfully applied to the determination of macro-  
27  
28 and micronutrients in plant materials.<sup>21</sup> Its suitability to simultaneous multielemental  
29  
30 determinations combined with its high spatial resolution make  $\mu$ -EDXRF a versatile  
31  
32 screening tool for elemental mapping in plants.  
33  
34

35  
36 Recently, a benchtop  $\mu$ -EDXRF instrument was used for investigating the Al<sup>22</sup>  
37  
38 spatial distribution in leaves of plants from High Altitude Rocky Complexes, Southeast  
39  
40 Brazil. Synchrotron radiation micro X-ray fluorescence spectrometry (SR- $\mu$ -XRF) was  
41  
42 also successfully used for mapping As,<sup>23</sup> Tl,<sup>24</sup> Pb,<sup>25</sup> Cd,<sup>26</sup> Se<sup>27</sup> and Zn<sup>28,29</sup> in  
43  
44 hyperaccumulator plants.<sup>30</sup>  
45  
46

47  
48 Some studies have investigated both the As spatial distribution and its speciation in  
49  
50 *Pteris vittata*.<sup>31-36</sup> Regarding *P. calomelanos*, there are important contributions dealing  
51  
52 with arsenic mapping,<sup>37,38</sup> however, to the best of the authors' knowledge, there are no  
53  
54 studies on simultaneous arsenic and phosphorus mapping in this fern species. This issue  
55  
56 deserves special attention because it has been demonstrated that arsenate exhibits a  
57  
58  
59  
60

1  
2  
3 strong physiological competition by the phosphate uptake systems in higher plants<sup>39</sup>,  
4  
5 but interference of As in P metabolism of hyperaccumulator ferns remains as a  
6  
7 controversial issue.<sup>40</sup>  
8

9  
10 In the present contribution,  $\mu$ -EDXRF was evaluated for the simultaneous As and P  
11  
12 microchemical mapping in sporophytes of *Pityrogramma calomelanos* grown in  
13  
14 absence and in As-enriched solutions. Moreover, the validation of a  $\mu$ -EDXRF method  
15  
16 for the quantitative determination of As and P in pelletized powdered fern samples is  
17  
18 presented.  
19

## 20 21 22 23 **Experimental**

24  
25  
26 Sporophytes of *Pityrogramma calomelanos* L. (Link) (Pteridaceae) were  
27  
28 obtained through *in vitro* culture of spores, and subsequently gametophytes, in  
29  
30 Murashige and Skoog (MS) medium.<sup>41</sup> The young sporophytes were cultivated in  
31  
32 commercial substrate Plantmax<sup>®</sup> in a greenhouse of the Plant Growth Unit at  
33  
34 Universidade Federal de Viçosa, Minas Gerais state, Brazil, at  $25 \pm 5$  °C. Ferns at 4-5  
35  
36 frond stage (n = 10) were transferred to a hydroponic system with half-strength  
37  
38 Hoagland nutrient solution,<sup>42</sup> pH 5.5, under continuous aeration. After an  
39  
40 acclimatization period of 4 weeks, the Hoagland nutrient solution containing  $1.0 \times 10^{-3}$   
41  
42 mol L<sup>-1</sup> As was used with half of the ferns. Arsenic was supplied as sodium arsenate  
43  
44 ( $\text{Na}_2\text{HAsO}_4 \cdot 7\text{H}_2\text{O}$ ). The remaining ferns were grown in Hoagland nutrient solution<sup>42</sup>  
45  
46 without As (control). There were five replicates per treatment and each replicate  
47  
48 involved a 2.2 L pot containing one plant. Plants were exposed during 21 days and the  
49  
50 solution was renewed weekly. Similarly, a second experiment with ferns at 5-7 frond  
51  
52 stage (n = 20, five replicates per treatment) were carried out in the absence and in the  
53  
54 presence of 1.0, 10 and  $30 \times 10^{-3}$  mol L<sup>-1</sup> As, under the same exposure time.  
55  
56  
57  
58  
59  
60

1  
2  
3 At the end of the experiments, pinnae, stipes, and roots were sampled, washed  
4 with deionized water and oven-dried at 60 °C until constant weight. In order to obtain  
5 flat surfaces required for elemental mapping, previously dried pinna samples were  
6 manually pressed between two decontaminated glass plates.  
7  
8  
9  
10

### 11 12 13 14 **ICP OES analysis**

15  
16  
17 Dried samples were powdered in a ball mill and sieved through a 200-mesh (74  
18  $\mu\text{m}$ ) stainless steel sieve. The sieved material (test sample for ICP OES) was accurately  
19 weighed (*ca.* 50 mg) in triplicate in closed TFM<sup>®</sup> digestion vessels (ETHOS 1600,  
20 Milestone, Italy). To each vessel, 5.0 mL of 2.8 mol L<sup>-1</sup> HNO<sub>3</sub> and 2.0 mL of H<sub>2</sub>O<sub>2</sub> 30  
21 % m m<sup>-1</sup> were added. The microwave heating program is shown in Table 1. After  
22 cooling to room temperature, the final solutions were transferred to volumetric flasks  
23 and the volume was made up to 10 mL with deionized water. The resulting digests were  
24 analyzed by ICP OES, with a dual view iCAP 6500 Duo optical emission spectrometer  
25 (Thermo Scientific, Waltham, MA, USA) equipped with a cyclonic spray chamber and  
26 a PEEK Mira Mist<sup>®</sup> nebulizer from the same manufacturer. The following ICP OES  
27 measurement conditions were used: 27 MHz generator frequency; 1.2 kW RF applied  
28 power; 1.5 mL min<sup>-1</sup> sample flow rate; 12, 0.5 and 0.6 L min<sup>-1</sup> argon flow rates for  
29 plasma, auxiliary and nebulizer, respectively; 15 s measurement time. Arsenic and  
30 phosphorus emission lines (As I 197.262 nm and P I 213.618 nm) were monitored in the  
31 axial and radial viewing mode, respectively.  
32  
33  
34  
35  
36  
37  
38  
39  
40  
41  
42  
43  
44  
45  
46  
47  
48  
49  
50

### 51 52 53 **$\mu$ -EDXRF analysis**

54  
55  
56  $\mu$ -EDXRF analysis were performed using a benchtop spectrometer ( $\mu$ EDX-1300,  
57 Shimadzu, Kyoto, Japan) furnished with a Rh X-ray tube with polycapillary lenses as  
58  
59  
60

1  
2  
3 X-ray convergence method, and a Si(Li) semiconductor detector (with 30 mm<sup>2</sup> detection  
4 area) sealed with a 8 μm thick Be window. The whole spectra comprised 4096 channels  
5 with a resolution of approximately 150 eV (FWHM) at 5.9 keV. Spectrum energy  
6 calibration was daily performed before each analysis batch by using an aluminum alloy  
7 (A 750 calibration standard). This was done for adjusting offset and system conversion  
8 gain (10 eV/channel) parameters.  
9

10  
11  
12  
13  
14  
15  
16 The limits of detection (LODs) were calculated as  $3.3 \times \frac{s}{b}$ , where  $s$  is the  
17 estimated standard deviation from the background (BG) intensity of each Kα peak (P  
18 Kα 2.01 keV and As Kα 10.54 keV) from the spectra of 10 pelletized pinna test  
19 samples. In each pellet 30 different test portions were irradiated (50 μm X-ray spot  
20 size). The BG intensities were calculated by the equipment software. The term “b” in  
21 the expression for LOD calculation is the slope of the calibration curve.  
22  
23  
24  
25  
26  
27  
28  
29  
30  
31

### 32 **Pellet preparation and method calibration**

33  
34  
35 Pellets of pinna, stipe, and root were prepared in a pneumatic press (Perkin  
36 Elmer, Waltham, MA, EUA) from previously ground and sieved samples by  
37 transferring 0.2 g of each sieved portion to a 13 mm internal diameter stainless steel die  
38 set and applying 8 t cm<sup>-2</sup> for 5 min. Pellets with approximately 1 mm thickness were  
39 used as test samples for μ-EDXRF quantitative analysis. Fourteen ground and sieved  
40 samples were selected from each fern part (pinna, stipe and root) totalizing 42 pellets  
41 (test samples).  
42  
43  
44  
45  
46  
47  
48  
49  
50

51 Three lines, comprising 30 measurement points each, were randomly selected on  
52 the pellet surface. Each measurement point (50 μm X-ray spot size) was analyzed  
53 during 10 s by keeping 100-μm distance between two adjacent sampling sites. The  
54 operational conditions are shown in Table 2.  
55  
56  
57  
58  
59  
60



1  
2  
3 Linear regression models were calculated to correlate As and P mass fractions  
4 determined by ICP OES with the corresponding  $K\alpha$  lines intensities ( $\text{cps } \mu\text{A}^{-1}$ ), as  
5 recommended elsewhere,<sup>21</sup> using either the data from all test samples ( $n = 42$ ) and also  
6 separately for each fern part ( $n = 14$ ).  
7  
8  
9  
10

### 11 12 13 14 **Microchemical As and P mapping**

15  
16  
17 Regarding microchemical mapping, the selected fern parts were horizontally  
18 fixed with adhesive tape onto a 4  $\mu\text{m}$  thick Mylar film previously assembled in an XRF  
19 sample cup, which was placed in a sample holder specially designed for transmitted  
20 image measurements. Sampling areas of 4 mm x 3 mm (80 x 60 measurement points; 50  
21  $\mu\text{m}$  step per site) were selected on the basal and apical portions of a pinnule, including  
22 the pinna midrib for simultaneous As and P mapping. Pinna samples with similar  
23 thickness and position in the stipe were chosen. A sampling area of 10 mm x 7.5 mm  
24 (200 x 150 measurement points; 50  $\mu\text{m}$  step per site) embracing the whole pinnules,  
25 attached to the pinna midrib, was also mapped. The following peaks: P  $K\alpha$  2.01 keV, As  
26  $K\alpha$  10.54 keV and Rh  $K\alpha$  Compton 18.96 keV were monitored for the construction of  
27 each microchemical map.  
28  
29  
30  
31  
32  
33  
34  
35  
36  
37  
38  
39  
40  
41

42 The following measurement conditions were used for mapping: 200  $\mu\text{A}$  and 50  
43 kV for X-ray tube current and voltage, respectively and *ca.* 10 % detector dead time.  
44 The elemental mapping was performed in three different pinnule samples (either for  
45 basal or apical portions) of both As-treated pinna and the control pinna. In order to  
46 circumvent the intermediate-thickness sample effect, which may affect the As detection  
47 in the analyzed matrix, the scattered radiation method was used.<sup>43,44</sup> In this case, the Rh  
48  $K\alpha$  Compton peak was selected as internal standard to compensate for the inherent  
49 differences in thickness and density along the mapped pinna regions. The software  
50  
51  
52  
53  
54  
55  
56  
57  
58  
59  
60

1  
2  
3 SigmaPlot® version 11 (San Jose, CA, USA) was used for the construction of the  
4  
5 microchemical maps.  
6

7 The mapped pinnule samples by  $\mu$ -EDXRF were photographed with a stereo  
8  
9 microscope (SZX7 Olympus) equipped with an EVOLT E-300 Olympus digital camera  
10  
11 (Olympus Optical). Figure 1 illustrates the morphological characteristics of *P.*  
12  
13 *calomelanos* highlighting the assayed pinna regions.  
14  
15

### 16 17 18 **Estimation of mass *per unit area* of pinna regions**

19  
20 Mass *per unit area* ( $\text{g cm}^{-2}$ ) of selected pinna regions (midrib and pinnule blade)  
21  
22 were estimated by weighing portions of midrib and pinnule blades and determining the  
23  
24 area of the selected portions by using the software Image-Pro Plus® version 4.5  
25  
26 (Rockville, MD, USA). This procedure was performed in triplicate.  
27  
28  
29

### 30 31 32 **Statistical analysis**

33  
34 The software Origin version 8 (Northampton, MA, USA) was used to perform  
35  
36 the linear regression analysis. For each linear regression model, the corresponding linear  
37  
38 correlation coefficient ( $r$ ) and the root mean square error of prediction (RMSEP) were  
39  
40 calculated as described elsewhere.<sup>45</sup>  
41  
42  
43  
44

### 45 46 47 **Results and discussion**

#### 48 49 50 **Determination of As and P by ICP OES**

51  
52 The quality of the measurements of As and P made by ICP OES after  
53  
54 microwave-assisted acid digestion (reference method) was checked by determining the  
55  
56 mass fraction of arsenic in the certified reference material BCR-060 (*Lagarosiphon*  
57  
58  
59  
60

1  
2  
3 *major*), and also the mass fractions of phosphorus in NIST SRM 1515 (Apple leaves)  
4  
5 and NIST SRM 1547 (Peach leaves). No significant differences were observed between  
6  
7 the certified and found values after applying the Student's *t*-test at 95 % confidence  
8  
9 level.  
10

11 *Pityrogramma calomelanos* ferns from the control treatment presented arsenic  
12 mass fractions of 1.6 to 2.7 mg kg<sup>-1</sup> for pinna and stipe, and of 9 to 52 mg kg<sup>-1</sup> for roots.  
13  
14 Ferns exposed to different As doses presented arsenic mass fractions ranging from 580  
15  
16 to 8800 mg kg<sup>-1</sup> in pinnae, 70 to 6600 mg kg<sup>-1</sup> in stipes, and 200 to 7800 mg kg<sup>-1</sup> in  
17  
18 roots. Higher As mass fractions were noted for the pinna from ferns exposed to 10 and  
19  
20 30 x 10<sup>-3</sup> mol L<sup>-1</sup> As that also presented apical and marginal necrosis in the old fronds.  
21  
22

23  
24 The phosphorus mass fractions ranged from 3.8 to 11 g kg<sup>-1</sup> in pinnae, 2.4 to 4.2  
25  
26 g kg<sup>-1</sup> in stipes, and 3.8 to 6.6 g kg<sup>-1</sup> in roots. In the first experiment, As promoted  
27  
28 diminution of P contents in ferns, but no appreciable changes were observed in the  
29  
30 samples from the second experiment. Ferns at 5-7 frond stage have probably a high  
31  
32 capacity to maintaining P status in roots and pinnae than younger ferns.  
33  
34  
35  
36  
37

### 38 **μ-EDXRF analysis of pelletized samples**

39

40  
41 A fragment of a typical μ-EDXRF spectrum obtained from the analysis of a  
42  
43 pelletized pinna of *P. calomelanos* is shown in Figure 2. Fragments of the spectra  
44  
45 containing the characteristic Kα peaks of As and P from the analysis of pelletized test  
46  
47 samples of pinnae were used to estimate the limits of detection (LODs) of 103 mg kg<sup>-1</sup>  
48  
49 As and 1.0 g kg<sup>-1</sup> P by μ-EDXRF. Limits of quantification (LOQs) of 309 mg kg<sup>-1</sup> As  
50  
51 and 3.0 g kg<sup>-1</sup> P were estimated as three times the obtained LODs.<sup>21</sup>  
52  
53  
54

55 Figure 3 shows the linear regression models calculated from the emission line  
56  
57 intensities of As Kα 10.54 keV and P Kα 2.01 keV, and their corresponding elemental  
58  
59  
60

1  
2  
3 mass fractions ( $\text{mg kg}^{-1}$  As and  $\text{g kg}^{-1}$  P) found in the pressed pellets of all fern  
4  
5 materials, with linear correlation coefficients ( $r$ ) higher than 0.98 ( $n = 42$ ) for both As  
6  
7 and P calibration models. The higher RMSEP values obtained for phosphorus (as high  
8  
9 as  $1230 \text{ mg kg}^{-1}$  P) in relation to arsenic (from 227 to  $671 \text{ mg kg}^{-1}$  As) can be derived  
10  
11 from the lower XRF sensitivity and, consequently, higher LOD values for the detection  
12  
13 of low atomic number elements.<sup>46</sup>  
14  
15

16  
17 The regression models were even better when pelletized powdered samples from  
18  
19 the same fern parts were used for calibration. This behavior was confirmed by better  
20  
21 RMSEP values and linear correlation coefficients when this calibration strategy was  
22  
23 used. As the RMSEP values represent an estimation of the predictive capacity of the  
24  
25 calibration models, their lowest values are a good indication that possible matrix effects  
26  
27 were minimized.  
28

29  
30 In general, the coefficients of variation of  $\mu$ -EDXRF measurements carried out  
31  
32 in all pelletized fern test samples varied from 1.0 to 17 % ( $n = 3$  sampling lines, 30 sites  
33  
34 per line,  $50 \mu\text{m}$  X-ray spot size).  
35

36  
37 It should be pointed out that, in addition to the abovementioned figures of merit,  
38  
39 one shall consider that the intensities of the characteristic X-ray emission lines of Ca, K,  
40  
41 S, Fe and Mn (Figure 2) can be similarly correlated with their corresponding mass  
42  
43 fractions in the pelletized fern materials, as already demonstrated for macro- and  
44  
45 micronutrients with pellets of powdered sugar cane leaves.<sup>21</sup>  
46  
47

### 48 49 50 **Microchemical mapping**

51  
52  
53 Microchemical qualitative maps were obtained in order to investigate As and P  
54  
55 distribution patterns in the pinna. To evaluate the necessity for applying the correction  
56  
57 strategy based on the scattered radiation method,<sup>43,44</sup> the data generated from the mass  
58  
59  
60

1  
2  
3 *per* unit area of the assayed pinna regions were compared with theoretical data, which  
4 were calculated with the equations described elsewhere<sup>47</sup> by using cellulose as the  
5 sample matrix.  
6  
7

8  
9 The final values obtained with the help of the aforementioned equations<sup>47</sup> were  
10 corrected taking into consideration the angle between the energy dispersive detector  
11 axis and the plane of the test sample. Based on this, a cellulose matrix can be considered  
12 thick at mass *per* unit area higher than about 0.01 g cm<sup>-2</sup> for phosphorus (P K $\alpha$  2.01  
13 keV) and approximately 1 g cm<sup>-2</sup> for arsenic (As K $\alpha$  10.54 keV). In the present study,  
14 the estimated mass *per* unit area was 0.0093  $\pm$  0.0002 g cm<sup>-2</sup> for the pinnule blade and  
15 0.025  $\pm$  0.005 g cm<sup>-2</sup> for the pinna midrib. Therefore, the scattered radiation method  
16 based on the use of the Rh K $\alpha$  Compton peak as internal standard was applied only for  
17 arsenic.  
18  
19

20  
21 Arsenic maps for control samples did not show any significant distribution trend  
22 in both basal and apical analyzed areas (Figure 4). In the basal portion of pinnule from  
23 ferns treated with 30 x 10<sup>-3</sup> mol L<sup>-1</sup> As, it was observed a preferential As localization in  
24 the pinna midrib and in the secondary ribs (Figure 4 a, As K $\alpha$ /Rh K $\alpha$  Compton map).  
25 The apical portion of pinnules from the 30 x 10<sup>-3</sup> mol L<sup>-1</sup> As treated fern also showed a  
26 preferential accumulation of As in the vascular regions (Figure 4 b, As K $\alpha$ /Rh K $\alpha$   
27 Compton map). Additionally, the As K $\alpha$ /Rh K $\alpha$  Compton maps obtained for whole  
28 pinnules indicated an increased gradient of the metalloid towards the margin, being the  
29 pinna tip the main As hotspot (Figure 5).  
30  
31

32  
33 Phosphorus distributions between vascular and non-vascular areas were similar  
34 for ferns of both treatments. Control and As-treated samples showed a high P  
35 concentration in internerval regions, which represent the photosynthetic areas, and a low  
36 P concentration in the pinna midrib and pinnule veins, which can be considered as As  
37  
38  
39  
40  
41  
42  
43  
44  
45  
46  
47  
48  
49  
50  
51  
52  
53  
54  
55  
56  
57  
58  
59  
60

1  
2  
3 hotspots (Figure 4). The same tendency was observed when comparing As and P maps  
4  
5 of whole As-treated pinnules (Figure 5). As-treated ferns showed a higher P  
6  
7 concentration in the basal portion of the pinnule whereas control samples presented a  
8  
9 higher P concentration in the apical region (Figure 4). A possible explanation for these  
10  
11 results is addressed in the next comments.  
12

### 13 14 15 16 **Comments on As and P localization in ferns compartments**

17  
18  
19 The importance of the proposed method for simultaneously investigating the  
20  
21 distribution of arsenic and phosphorus in the As-hyperaccumulator fern *Pityrogramma*  
22  
23 *calomelanos* by  $\mu$ -EDXRF is further demonstrated by briefly commenting and  
24  
25 suggesting possible mechanisms for explaining the results reported here.  
26

27  
28 Arsenic was not detected in the control samples, indicating that the mass  
29  
30 fractions were below the estimated LOD ( $103 \text{ mg kg}^{-1} \text{ As}$ ). In As-treated ferns, arsenic  
31  
32 was preferentially located along the veins and in the apical and marginal regions of the  
33  
34 pinna, in accordance with previous report for *Pteris vittata*.<sup>33</sup> This distribution pattern  
35  
36 corroborates with the mechanism of As transport from root to shoot, which is driven by  
37  
38 transpiration, similarly to several other elements.<sup>48,49</sup> Arsenic is transported through  
39  
40 xylem to the lamina of the frond, where it seems to be sequestered in the vacuole.<sup>50</sup>  
41  
42

43  
44 Arsenate is the dominant As species in aerobic soils.<sup>51</sup> In *Pteris vittata*, arsenate  
45  
46 is the main As species transported through the xylem sap when arsenic is supplied as an  
47  
48 inorganic form.<sup>52</sup> Francesconi *et al.*<sup>12</sup> analyzed *Pityrogramma calomelanos* ferns grown  
49  
50 in an As-contaminated soil (presenting 6-12 % of water-extractable As with 97 % of  
51  
52 this as arsenate). The ferns presented 60 % of water-extractable arsenic from their  
53  
54 rhizoids, and the largest fraction (95 %) as arsenate. Once arsenate is uptaken by fern  
55  
56 roots, most of it can be reduced to arsenite, mainly in the frond.<sup>33,34</sup> Vacuolar  
57  
58  
59  
60

1  
2  
3 sequestration of arsenite represents a strategy for As detoxification in the  
4 hyperaccumulator ferns.<sup>51</sup> In the present study, the observed higher As accumulation  
5 pattern in pinna tissues may have caused toxic effects, as observed by the occurrence of  
6 brownish-orange necrotic areas in the pinna tip. This arsenic-mediated phytotoxicity  
7 may have induced the observed decay in the phosphorus content in the apical portion of  
8 the As-treated pinna (Figures 4 and 5, P K $\alpha$  maps). Similarly, Tu *et al.*<sup>53</sup> evaluated the  
9 effects of arsenate and phosphate on As and P accumulation patterns in roots and fronds  
10 of *P. vittata*. In this study<sup>53</sup> it was found a decrease in the phosphate accumulation in the  
11 roots and fronds at high arsenate doses. Another possible explanation for this behavior  
12 can be derived from the competition between arsenate and phosphate. In this sense, the  
13 P transport along the pinnule is impaired, thus dropping its concentration in the apical  
14 region.  
15  
16  
17  
18  
19  
20  
21  
22  
23  
24  
25  
26  
27  
28  
29  
30  
31

### 32 **Conclusions and outlook**

33  
34  
35 This is the first study to propose a validated analytical method using  $\mu$ -EDXRF  
36 for quantitative determination and mapping As and P simultaneously in *Pityrogramma*  
37 *calomelanos*, a well-recognized As-hyperaccumulator fern.  
38  
39  
40  
41

42 The analysis of pelletized powdered fern samples was also addressed as a  
43 powerful tool for plant nutrition diagnosis, as this information proved to be useful for  
44 explaining possible induced phosphorus deficiency in As-accumulating plants. The  
45 results obtained here demonstrate the usefulness of this method to detect  
46 bioaccumulation of As in plants, especially when cultivated in As-enriched soils or  
47 irrigated with contaminated water. In addition, in view of the presented results, further  
48 systematic studies on physiological mechanisms involved in As species and P  
49  
50  
51  
52  
53  
54  
55  
56  
57  
58  
59  
60

1  
2  
3 distribution in pinna tissues of *Pityrogramma calomelanos* L. (Link) under As exposure  
4  
5 are encouraged.  
6

7  
8 In short, the proposed strategy provides important information regarding  
9  
10 environmental monitoring and phytoremediation studies to be obtained in a fast and  
11  
12 non-destructive way.  
13

### 14 15 16 17 **Acknowledgements**

18  
19  
20 The authors are grateful to FAPEMIG (Foundation for Research Support of  
21  
22 Minas Gerais) for the doctoral scholarship of N. V. Campos and financial support to the  
23  
24 projects APQ-02070-11 and 12070/2009 and to CNPq (National Council for Scientific  
25  
26 and Technological Development) for providing research scholarship to A. A. Azevedo  
27  
28 (312190/2013-1), C. Schaefer and F. J. Krug (306679/2014-1). The authors also thank  
29  
30 the Fundação de Amparo à Pesquisa do Estado de São Paulo (FAPESP 2012/16203-5)  
31  
32 and to Dr. Eduardo de Almeida and Prof. Elias Ayres Guidetti Zagatto for critical  
33  
34 comments and language improvement.  
35  
36  
37  
38  
39  
40  
41  
42  
43  
44  
45  
46  
47  
48  
49  
50  
51  
52  
53  
54  
55  
56  
57  
58  
59  
60



**References**

1. B. K. Mandal and K. T. Suzuki, *Talanta*, 2002, **58**, 201–235.
2. M. F. Lengke, C. Sanpawanitchakit and R. N. Tempel, *Can. Mineral.*, 2009, **47**, 593–613.
3. D. B. Johnson and K. B. Hallberg, *Sci. Total Environ.*, 2005, **338**, 3–14.
4. A. Akcil and S. Koldas, *J. Clean Prod.*, 2006, **14**, 1139–1145.
5. P. L. Smedley and D. G. Kinniburgh, *Appl. Geochem.*, 2002, **17**, 517–568.
6. N. K. Niazi, B. Singh, L. Van Zwieten and A. G. Kachenko, *Environ. Sci. Pollut. Res.*, 2012, **19**, 3506–3515.
7. P. R. Baldwin and D. J. Butcher, *Microchem. J.*, 2007, **85**, 297–300.
8. J. T. Lessl and L. Q. Ma, *Environ. Sci. Technol.*, 2013, **47**, 5311–5318.
9. A. J. M. Baker and P. L. Walker, Ecophysiology of metal uptake by tolerant plants, in: A. J. Shaw, (Editor), Heavy metal tolerance in plants: evolutionary aspects, CRC, Boca Raton, 1990, pp 155–177.
10. N. Mganga, M. L. K. Manoko and Z. K. Rulangeranga, *Tanz. J. Sci.*, 2011, **37**, 109–119.
11. L. Q. Ma, K. M. Komar, C. Tu, W. Zhang, Y. Cai and E. D. Kennelley, *Nature*, 2001, **409**, 579.
12. K. Francesconi, P. Visoottiviseth, W. Sridokchan and W. Goessler, *Sci. Total Environ.*, 2002, **284**, 27–35.
13. X. Wan, M. Lei, Y. Liu, Z. Huang, T. Chen, D. Gao, *Sci. Total Environ.*, 2013, **442**, 143–151.
14. B. T. K. Anh, D. D. Kim, P. Kuschik, T. V. Tua, N. T. Hue, N. N. Minh, *J. Environ. Biol.*, 2013, **34**, 237–242.

- 1  
2  
3 15. D. E. Salt, R. D. Smith and I. Raskin, *Annu. Rev. Plant Physiol. Plant Mol. Biol.*,  
4 1998, **49**, 643–668.  
5  
6  
7 16. Y. P. Kalra, *Handbook of reference methods for plant analysis*, CRC Press, Boca  
8 Raton, FL, USA, 1998.  
9  
10  
11 17. P. Masson, T. Dalix, S. Bussière, *Commun. Soil Sci. Plant Anal.*, 2010, **41**, 231 –  
12 243.  
13  
14  
15 18. M. Hoenig, *Talanta*, 2001, **54**, 1021–1038.  
16  
17  
18 19. A. A. Shaltout, I. N. B. Castilho, B. Welz, E. Carasek, I. B. G. Martens, A. Martens,  
19 S. M. F. Cozzolino, *Talanta*, 2011, **85**, 1350-1356.  
20  
21  
22 20. R. M. Barnes, D. Santos Jr. and F. J. Krug, in *Microwave-Assisted Sample*  
23 *Preparation for Trace Element Determination*, ed. E. M. M. Flores, Elsevier,  
24 Amsterdam. 2014, pp. 1-58.  
25  
26  
27 21. M. B. B. Guerra, C. E. G. R. Schaefer, G. G. A. Carvalho, P. F. Souza, D. Santos Jr,  
28 L. C. Nunes and F. J. Krug, *J. Anal. At. Spectrom.*, 2013, **28**, 1096–1101.  
29  
30  
31 22. N. V. Campos, T. A. R. Pereira, M. F. Machado, M. B. B. Guerra, G. S. Tolentino,  
32 J. S. Araújo, M. Q. Rezende, M. C. N. A. Silva and C. E. G. R. Schaefer, *An. Acad.*  
33 *Bras. Cienc.*, 2014, **86**, 365–376.  
34  
35  
36 23. N. Kitajima, T. Kashiwabara, N. Fukuda, S. Endo, A. Hokura, Y. Terada and I.  
37 Nakai, *Chem. Lett.*, 2008, **37**, 32–33.  
38  
39  
40 24. K. G. Scheckel, E. Lombi, S. A. Rock and M. J. Mclaughlin, *Environ. Sci. Technol.*,  
41 2004, **38**, 5095–5100.  
42  
43  
44 25. H. Kodera, H. Nishioka, Y. Muramatsu and Y. Terada, *Anal. Sci.*, 2008, **24**, 1545–  
45 1549.  
46  
47  
48 26. N. Fukuda, A. Hokura, N. Kitajima, Y. Terada, H. Saito, T. Abe and I. Nakai, *J.*  
49 *Anal. At. Spectrom.*, 2008, **23**, 1068–1075  
50  
51  
52  
53  
54  
55  
56  
57  
58  
59  
60

- 1  
2  
3 27. J. L. Freeman, M. A. Marcus, S. C. Fakra, J. Devonshire, S. P. McGrath, C. F.  
4  
5 Quinn and E. A. H. Pilon-Smits, *PLoS One*, 2012, **7**, e50516.  
6  
7 28. L. Lu, S. Tian, J. Zhang, X. Yang, J. M. Labavitch, S. M. Webb, M. Latimer and P.  
8  
9 H. Brown, *New Phytol.*, 2013, **198**, 721–731.  
10  
11 29. L. Lu, X. Liao, J. Labavitch, X. Yang, E. Nelson, Y. Du, P. H. Brown and S. Tian,  
12  
13 *Plant Physiol. Biochem.*, 2014, **84**, 224–232.  
14  
15 30. M. J. Pushie, I. J. Pickering, M. Korbas, M. J. Hackett and G. N. George, *Chem.*  
16  
17 *Rev.* 2014, **114**, 8499–8541.  
18  
19 31. B. R. Bondada, R. S. Underhill, L. Q. Ma, Y. Guyodo, A. Mikhaylova, M. R.  
20  
21 Davidson, R. S. Duran, in *Arsenic in Soil and Groundwater Environment*, ed. P.  
22  
23 Bhattacharya, A. B. Mukherjee, J. Bundschuh, R. Zevenhoven, R. H. Loeppert,  
24  
25 Elsevier, Amsterdam. 2007, pp. 299-313.  
26  
27 32. E. Lombi, F. Zhao, M. Fuhrmann, L. Q. Ma and S. P. McGrath, *New Phytol.*, 2002,  
28  
29 **156**, 195–203.  
30  
31 33. A. Hokura, R. Omuma, Y. Terada, N. Kitajima, T. Abe, H. Saito, S. Yoshida and I.  
32  
33 Nakai, *J. Anal. At. Spectrom.*, 2006, **21**, 321–328.  
34  
35 34. I. J. Pickering, L. Gumaelius, H. H. Harris, R. C. Prince, G. Hirsch, J. A. Banks, D.  
36  
37 E. Salt and G. N. George, *Environ. Sci. Technol.*, 2006, **40**, 5010–5014.  
38  
39 35. T. Kashiwabara, A. Hokura, N. Kitajima, R. Onuma, H. Saito, T. Abe and I. Nakai,  
40  
41 *Bunseki Kagaku*, 2006, **55**, 743–748.  
42  
43 36. X.-M. Wan, M. Lei, X.-Y. Zhou, J. Yang, T. Chen and G.-D. Zhou, *Instrum. Sci.*  
44  
45 *Technol.*, 2014, **42**, 667–677.  
46  
47 37. A. G. Kachenko, M. Gräfe, B. Singh and S. M. Heald, *Environ. Sci. Technol.*, 2010,  
48  
49 **44**, 4735–4740.  
50  
51  
52  
53  
54  
55  
56  
57  
58  
59  
60

- 1  
2  
3 38. A. G. Kachenko, N. P. Bhatia, B. Singh and R. Siegele, *Plant Soil*, 2007, **300**, 207–  
4 219.  
5  
6  
7 39. C. I. Ullrich-Eberius, A. Sanz and A. J. Novacky, *J. Exp. Bot.*, 1989, **40**, 119–128.  
8  
9  
10 40. Z. -C. Huang, Z. -Z. An, T. -B. Chen, M. Lei, X. -Y. Xiao and X. -Y. Liao, *J.*  
11 *Environ. Sci.*, 2007, **19**, 714–718.  
12  
13  
14 41. T. Murashige and F. Skoog, *Physiol. Plantarum*, 1962, **15**, 473–497.  
15  
16 42. D.R. Hoagland and D.I. Arnon, The water-culture method for growing plants  
17 without soil, California Agricultural Experiment Station, Berkeley, 1950.  
18  
19  
20 43. E. Marguá, I. Queralt, M. Hidalgo, *Trends Anal. Chem.*, 2009, **28**, 362-372.  
21  
22  
23 44. R. C. Reynolds Jr., *Am. Mineral.*, 1963, **48**, 1133-1143.  
24  
25 45. M. B. B. Guerra, E. Almeida, G. G. A. Carvalho, P. F. Souza, L. C. Nunes, D.  
26 Santos Júnior and F. J. Krug, *J. Anal. At. Spectrom.*, 2014, **29**, 1667–1674.  
27  
28  
29 46. M. S. Blonski, C. R. Appoloni, P. S. Parreira, P. H. A. Aragão and V. F. Nascimento  
30 Filho, *J. Radioanal. Nucl. Chem.*, 2006, **270**, 197–201.  
31  
32  
33 47. Bruker Corporation. What Does “Infinite Thickness” Mean in Reference to XRF?  
34 Available at: [https://www.bruker.com/pt/products/x-ray-diffraction-and-elemental-](https://www.bruker.com/pt/products/x-ray-diffraction-and-elemental-analysis/handheld-xrf/infinite-thickness-xrf-analysis.html)  
35 [analysis/handheld-xrf/infinite-thickness-xrf-analysis.html](https://www.bruker.com/pt/products/x-ray-diffraction-and-elemental-analysis/handheld-xrf/infinite-thickness-xrf-analysis.html). Accessed on September  
36 2015.  
37  
38  
39  
40  
41  
42 48. H. Marschner, Mineral nutrition of higher plants, London, Academic Press, 1986,  
43 674p.  
44  
45  
46 49. X. -M Wan, M. Lei, T. -B Chen, J. -X Yang, H. -T Liu and Y. Chen, *Environ. Sci.*  
47 *Pollut. Res.*, 2015, in press, DOI 10.1007/s11356-015-4746-6.  
48  
49  
50  
51 50. E. Indriolo, G -N. Na, D. Ellis, D. E. Salt and J. A. Banks, *Plant Cell*, 2010, **22**,  
52 2045–2057.  
53  
54  
55 51. F. J. Zhao, J. F. Ma, A. A. Meharg and S. P. McGrath, *New Phytol.*, 2009, **181**, 777–  
56 794.  
57  
58  
59  
60

- 1  
2  
3 52. G. M. Kertulis, L. Q. Ma, G. E. MacDonald, R. Chen, J. D. Winefordner and Y. Cai,  
4  
5 *Environ. Exp. Bot.*, 2005, **54**, 239–247.  
6  
7 53. C. Tu, L. Q. Ma, *Plant Soil*, 2003, **249**, 373–382.  
8  
9  
10  
11  
12  
13  
14  
15  
16  
17  
18  
19  
20  
21  
22  
23  
24  
25  
26  
27  
28  
29  
30  
31  
32  
33  
34  
35  
36  
37  
38  
39  
40  
41  
42  
43  
44  
45  
46  
47  
48  
49  
50  
51  
52  
53  
54  
55  
56  
57  
58  
59  
60

**Tables**

Table 1. Microwave heating program for plant acid digestions

Step	Time (min)	Target temperature (°C)	Condition
1	3	160	Ramping
2	2	-	No heating
3	5	200	Ramping
4	15	200	Holding

Table 2.  $\mu$ -EDXRF operational conditions

Instrumental parameter	Operating condition
Irradiated diameter	50 $\mu$ m
Measurement time for pellet interrogation	300 s
Analyzed spectra region	1– 40 keV
Measuring atmosphere	Atmospheric air
Monitored peaks	P $K\alpha$ 2.01 keV, As $K\alpha$ 10.54 keV and Rh $K\alpha$ Compton 18.96 keV
X-ray tube voltage	50 kV
X-ray tube current for pellet interrogation	100 $\mu$ A
Maximum sample size	200 (W) x 300 (D) x 40 (H) mm
Maximum stroke	X-Y - 100 mm x 100 mm Z - 40 mm

**Captions for figures**

Figure 1. Morphological characteristics of *P. calomelanos* emphasizing the pinna regions used for arsenic and phosphorus microchemical mapping by  $\mu$ -EDXRF. (a) Sporophyte. (b) Pinna. (c) Basal portion of the pinnule and (d) Apical portion of the pinnule.

Figure 2. Fragment of typical  $\mu$ -EDXRF spectrum related to a pressed pellet of pinna of *P. calomelanos* with  $1600 \text{ mg kg}^{-1}$  As and  $11 \text{ g kg}^{-1}$  P. Experimental conditions:  $50 \mu\text{m}$  spot size and 300 s measurement time.

Figure 3. Linear regression models adjusted to correlate As (a-d) and P (e-h) mass fractions determined by ICP OES and  $\mu$ -EDXRF intensity ( $\text{cps } \mu\text{A}^{-1}$ ). Data from all samples and separately for each fern part (pinna, stipe and root).

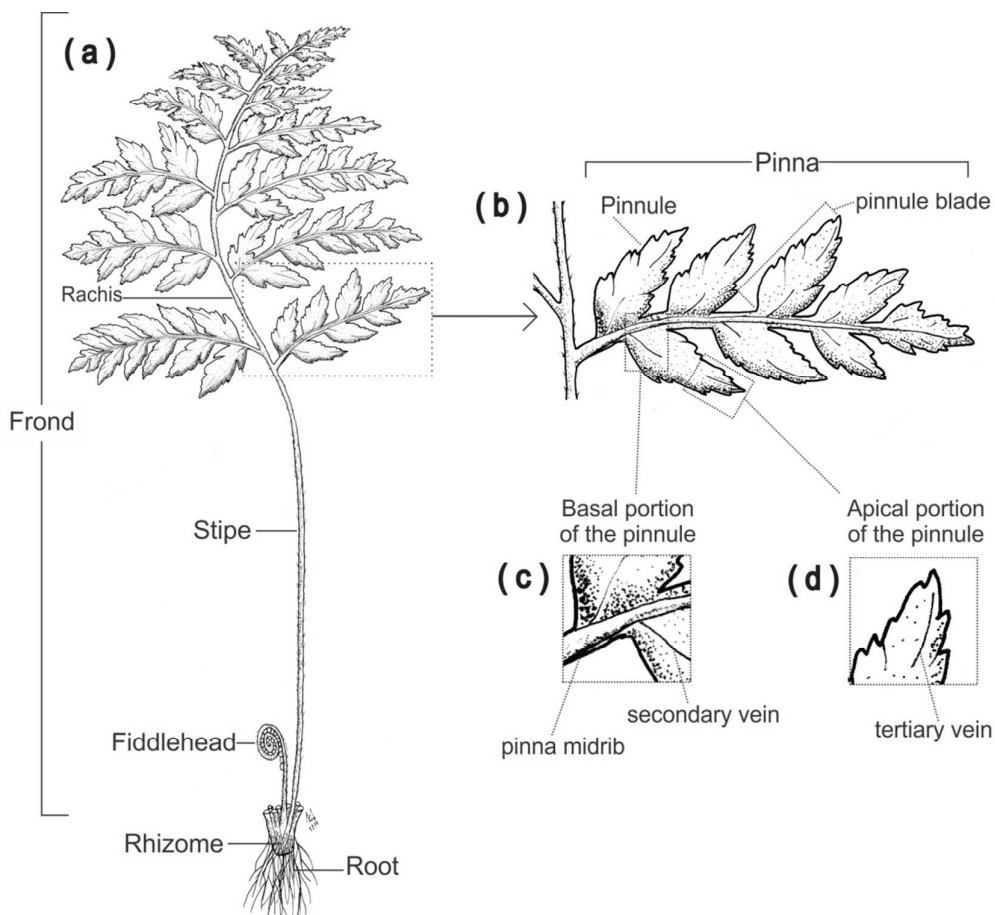
Figure 4.  $\mu$ -EDXRF microchemical maps for As and P of the basal (a) and apical (b) portions of the pinnule of *Pityrogramma calomelanos* from control ferns and ferns exposed to  $30 \times 10^{-3} \text{ mol L}^{-1}$  As. For As maps the Rh  $K\alpha$  Compton peak was used as internal standard. Legend: pm = pinna midrib; sv = secondary vein. Arrow = tertiary ribs. Bars length = 1.0 mm. Experimental conditions:  $50 \mu\text{m}$  spot size and 120 min. irradiation time.

Figure 5.  $\mu$ -EDXRF microchemical maps for As and P of whole pinnules of *Pityrogramma calomelanos* ferns exposed to  $30 \times 10^{-3} \text{ mol L}^{-1}$  As. For As maps the Rh



1  
2  
3 K $\alpha$  Compton peak was used as internal standard. Bars length = 2.0 mm. Experimental  
4  
5 conditions: 50  $\mu\text{m}$  spot size and 750 min. irradiation time.  
6  
7  
8  
9  
10  
11  
12  
13  
14  
15  
16  
17  
18  
19  
20  
21  
22  
23  
24  
25  
26  
27  
28  
29  
30  
31  
32  
33  
34  
35  
36  
37  
38  
39  
40  
41  
42  
43  
44  
45  
46  
47  
48  
49  
50  
51  
52  
53  
54  
55  
56  
57  
58  
59  
60

Figure 1



1  
2  
3  
4  
5  
6  
7  
8  
9  
10  
11  
12  
13  
14  
15  
16  
17  
18  
19  
20  
21  
22  
23  
24  
25  
26  
27  
28  
29  
30  
31  
32  
33  
34  
35  
36  
37  
38  
39  
40  
41  
42  
43  
44  
45  
46  
47  
48  
49  
50  
51  
52  
53  
54  
55  
56  
57  
58  
59  
60

Figure 2

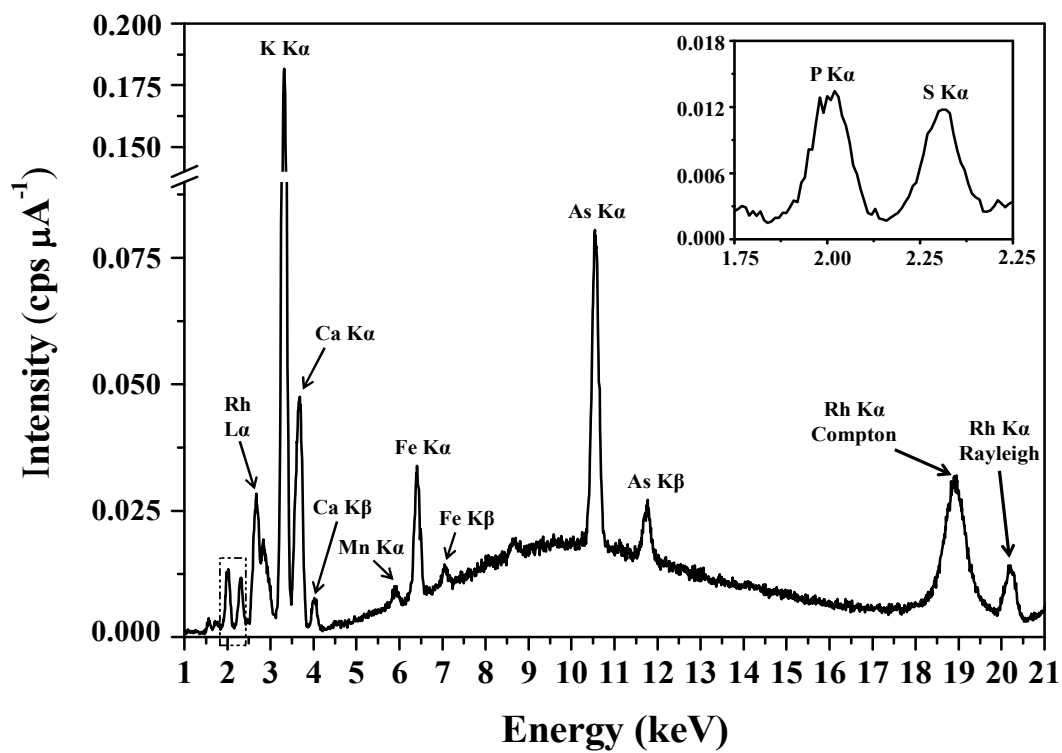
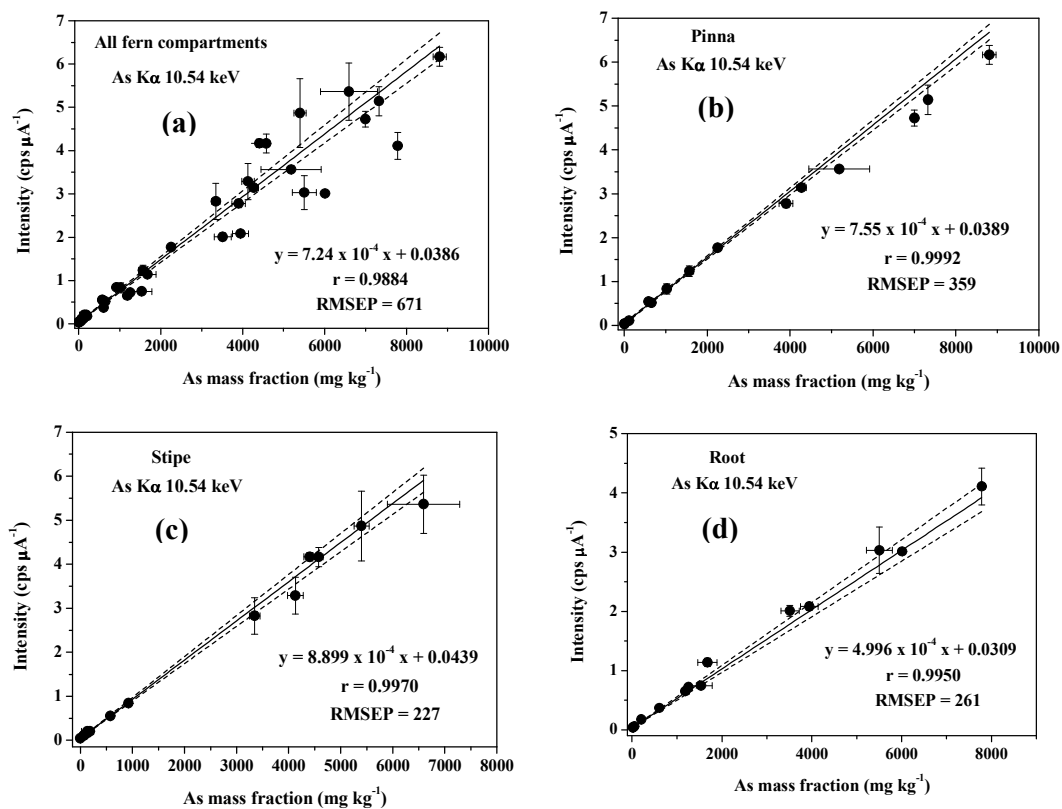


Figure 3



Continuation... Figure 3

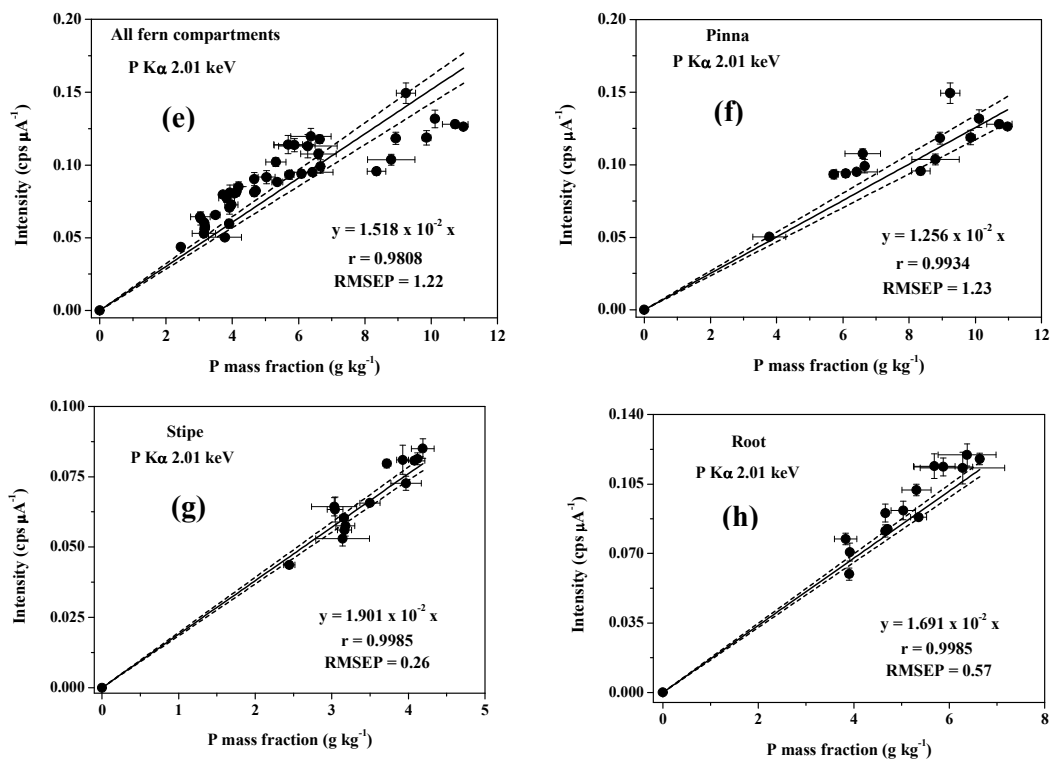


Figure 4

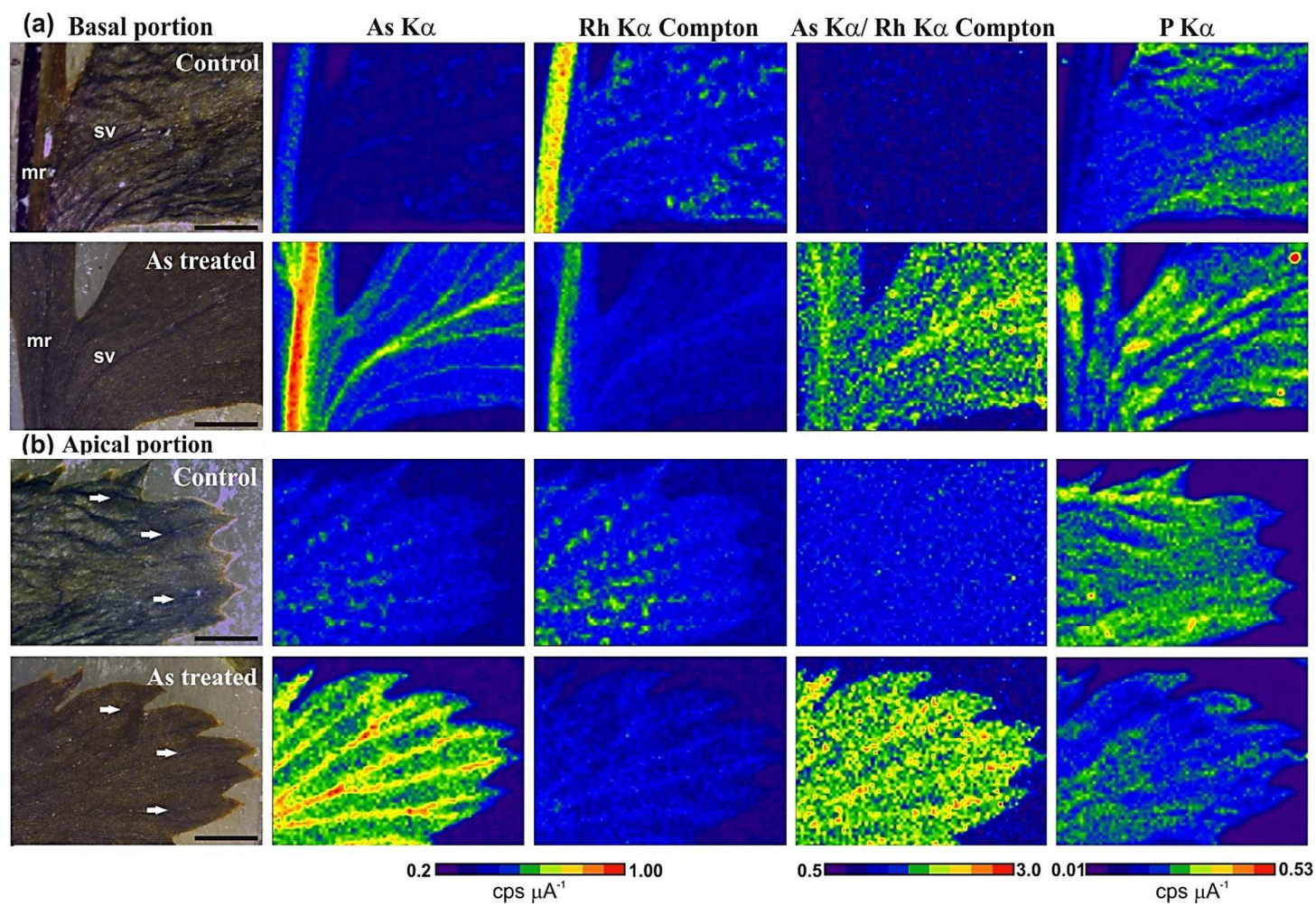
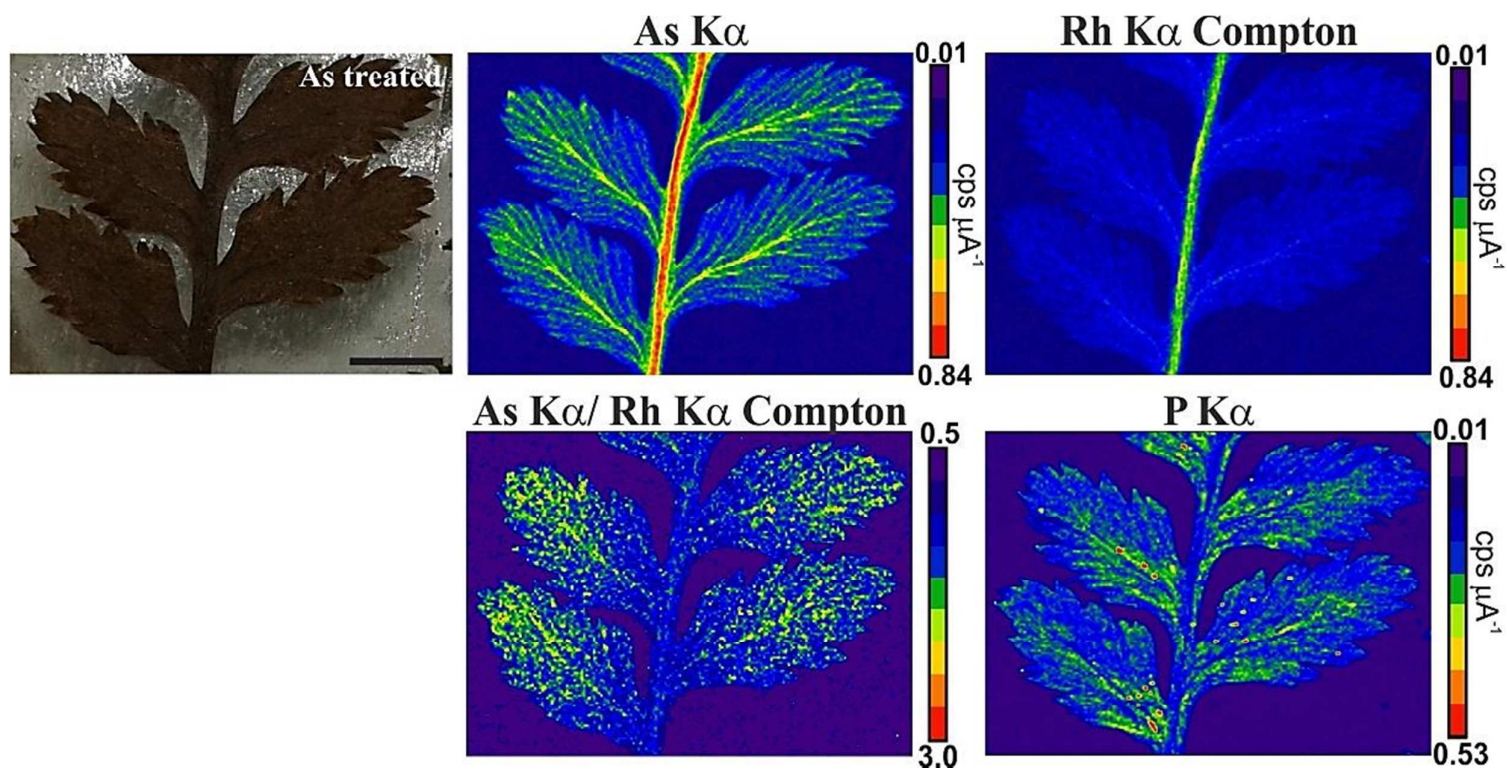
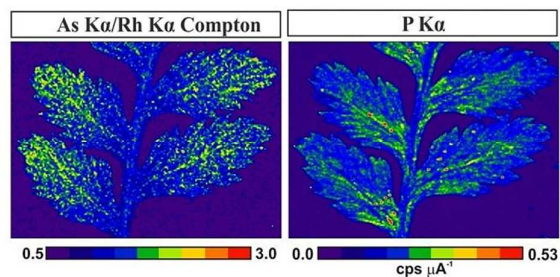


Figure 5





$\mu$ -EDXRF is a strong analytical tool enabling the simultaneous mapping of As and P in the As-hyperaccumulator fern *Pityrogramma calomelanos*.